

# Removed of Pollutants from aqueous solutions using ecologically acceptable products

Majed Kareem Abed<sup>1\*</sup>, M. M. Sirhan<sup>2</sup>

Researcher, Department of Chemistry, College of Education for Pure Sciences, University of Anbar,  
Ramadi, Iraq<sup>1</sup>

Assistant Professor, Department of Chemistry, College of Education for Pure Sciences, University of Anbar,  
Ramadi, Iraq<sup>2</sup>

Corresponding Author: 1\*



---

## Keywords:

Activated carbon, Bitter Melon, Adsorption, Chromium, lead.

---

## ABSTRACT

In light of the benefits that the Bitter Melon (*Momordica charantia*) may bring in terms of abundance, this research investigates the possibility of employing the Peels of the Bitter Melon in the manufacture of activated carbon. low cost and product quality. Bitter melon Peels were used to make activated carbon, which was then activated using the HNO<sub>3</sub> chemical activation procedure. FT-IR and SEM methods were used to determine surface characteristics. To test the produced carbon's potential to absorb Cr<sup>+3</sup>, Pb<sup>+2</sup> and PPD dyes, they were chosen as important chemical contaminants. The adsorption process was monitored and the elements that influenced it were investigated, including adsorbent mass, temperature, pH, contact time, and initial adsorbed material concentration. It was shown that the adsorption capacity of Cr<sup>+3</sup>, Pb<sup>+2</sup> and dye increased with decreasing temperature. For the adsorbents given, the optimal pH value was (pH= 5 and 6) and the best contact timeframe was (120 min). ΔG, ΔS and ΔH thermodynamic functions were determined. It was observed that the adsorption process is endothermic, since adsorption increases with increasing temperature, and that it is spontaneous. and a rise in randomness, implying that the adsorbent surface is less uniform than the solution. as well as a research study To remove tiny amounts of ions in vast volumes of aqueous solutions, the batch technique and the column method are used.

---



This work is licensed under a Creative Commons Attribution Non-Commercial 4.0 International License.

---

## 1. INTRODUCTION

Any anthropogenic substance that is disseminated or present in higher than usual proportions in the environment is referred to be a chemical pollution [1]. Over 100,000 chemicals are generated for commercial use, and many of them end up in the aquatic environment via the atmosphere, runoff, or direct discharge into water [2]. Chemical pollutants are dangerous not only because of their existence, but also because of the possibilities of interactions with species and other chemicals, as well as interactions with light and even live creatures [3]. In order to analyze chemical pollutants effectively, they are frequently divided into inorganic and organic pollutants based on their chemical structure [4]. Heavy metals, various types of nutrients, and

salts are examples of inorganic pollutants that occur naturally or as a result of human activity. Exposure to inorganic contaminants in water is typically a challenging task. Heavy metals, such as (Pb), have a varied behavior since they do not decompose like many organic contaminants do [5]. Inorganic pollutants in excess of the permissible limits can have a variety of negative consequences on the liver, kidneys, digestive system, and skin (depending on the level of exposure) [6]. Organic pollutants are harmful substances that contain carbon in their composition and have a global impact on human health and the environment because they are spread by water or wind and are not contained within the polluted region. It can accumulate in one species and be passed to another through the food chain, and it can last for a long period in the environment [7]. Because the dyes have a high water solubility, they are difficult to remove using traditional procedures. These dyes harm water bodies by preventing light from passing through, resulting in a reduction in the rate of photosynthesis and dissolved oxygen levels, hurting aquatic species as a whole [8]. The risk of para-phenylene diamine (PPD) hair dye is characterized by the fact that it causes the oxidation process to generate various intermediate chemicals that can induce significant allergic responses, mutagenicity, and are very poisonous (9). Because of its great efficiency and low cost, adsorption technology is regarded the most effective. It employs a variety of natural and synthetic adsorbents, including sugar cane, fruit peels, natural clay, and other agricultural wastes, as well as industrial wastes like gravel, fly ash, and activated carbon obtained from biological sources. For eliminating different contaminants from wastewater, nanomaterials based on minerals and other elements, zeolite-based adsorbents, and low-cost polymers are being developed [10].

Because there is a paucity of available and published information on activated carbon made from Bitter Melon, the purpose of this study is to investigate novel uses for this raw material in the purification of contaminated water.

## 2. Materials and methods

### 2.1 Materials and devices used

The FT-IR spectra were recorded on an Infrared spectrophotometer Model Tensor 27 Bruker Co., Germany as ATR technique. Atomic force microscope, scanning electron microscope, UV spectroscopy. All chemicals were purchased from Sigma-Aldrich, Nitric acid, Lead nitrate, Chromic nitrate, PPD, iodine, Methylene blue and distilled water, Bitter Melon (*Momordica charantia*). Preparation of the raw material: 1.5 kg of Bitter Melon were gathered and cleaned many times with distilled water to remove contaminants and suspended particles. It was allowed to dry at room temperature before being crushed into a fine powder using an electric mill with a diameter of (15 cm), sieved using a sieve with a hole size of 30-200  $\mu$ m, and dried in a drying oven at (60°C) for 48 hours.

### 2.2 Preparation of activated carbon with Nitric acid

The prepared powder was drenched in a glass beaker and nitric acid was added to it (10%). The powder was left to saturate with the solution for 24 hours until the mixture was homogeneous. The solution was filtered and the sample was washed with distilled water several times and dried at a temperature (100 °C) until the weight was stable. Then (20 g) of the prepared powder was calcined (carbonized) in five clean and closed earthenware lids in an oven at temperatures of (500, 600, 700, 800 and 900 °C) for one hour. Then crushed activated charcoal (AC) was washed several times with distilled water until the pH of the washing water became pH = 7, then dried at a temperature of (110°C) until the weight was stable. The five forms of activated charcoal were named nitric acid (CHN1, CHN2, CHN3, CHN4, and CHN5), respectively.

Characterization of activated carbon and raw material: FT-IR spectroscopy was used to determine the chemical surface functions of the various models of activated carbon and the raw material, and scanning

electron microscopy was used to diagnose the surface morphology (SEM).

### 2.2.1 Ash content and moisture

The ash content was determined by placing (0.5g) of dry activated carbon at (110°C) for 2 hours, then putting it in a crucible of defined mass and burning it for 3 hours at (800°C). After that, the proportion of ash is calculated using the following mathematical formula:

$$\% H = \frac{m_3 - m_2}{0.5} \times 100$$

Iodine index: The inner surface area of activated carbon was measured using a volumetric flask filled with 50 mL of iodine solution (0.02N) and 0.1g of activated carbon. Before sifting, the mixture was agitated for 10 minutes. The filtrate was collected and 10 mL was added to it. 2 drops of the starch solution was prepared in advance to obtain a purple solution. After volumetric doses of a standard sodium thiosulfate solution (0.1N) were created in the burette and the purple hue was changed to a colorless solution, the volume of sodium thiosulfate was determined, and the iodine index was computed using the following mathematical formula [11].

$$\text{Index } I_2 = \left( \frac{N_0 \times N_{th} \times V_{th}}{2 \times V_{I_2}} \right) \times \left( \frac{M_{I_2} \times V_{ads}}{m_{ac}} \right)$$

Methylene blue indicator: A measurement of activated carbon surface area, indicates the capacity of activated carbon to absorb large particles. 0.1g of activated carbon and 100 mL of methylene blue (MB) at a concentration of (25 mg/L) were mixed in a conical flask and placed in a vibrating water bath at (25°C) for 2 hours, after which the remaining (MB) concentration was measured and the (MB) index was calculated using the following mathematical formula [12].

$$\text{Index}_{(MB)} = \frac{C_i - C_f}{m_{ac}} \times 100$$

Zero charge point pH: (50 mL) distilled water was added to five flasks, and the pH was adjusted to (2,4,6,8, and 10) and then (0.05g) of activated carbon was added and stirred at room temperature until the pH stabilized and the final pH was determined, and (pH pzc) is calculated from the intersection of the curve that represents the relationship between the initial pH  $pH_i$  and the amount of pH change  $\Delta pH$ .

### 2.2.2 Study of the factors affecting adsorption

The effect of the adsorbent mass: Adding various weights of activated carbon samples (0.02,0.04,0.06,0.08, and 0.1g) to (50 mL) of (PPD), ( $Pb^{+2}$ ) and ( $Cr^{+3}$ ) at a concentration of (100 mg/L) and placing in a vibrating water bath at a temperature of (25°C) for 2 hours, the solution was filtered, the residual concentration measured, and the adsorption percentage was calculated using the following mathematical equation [13].

$$\% \text{ Removal} = \frac{C_0 - C_e}{C_0} \times 100$$

Effect of time on adsorption: Several solutions of (50 mL volume) with concentrations of (100 mg/L) of (PPD), ( $Pb^{+2}$ ) and ( $Cr^{+3}$ ), and (0.1g) of activated carbon were prepared and placed in a vibrating water bath at (25°C) for different times (10, 25, 40, 90, 120, 150 and 180 minutes), filtering the solution after the specified time and measuring the remaining concentration, and the amount of adsorption was calculated at each time  $Q_t$  from the following equation [14].

$$Q_t = \frac{(C_0 - C_t)}{m_{ac}} \cdot V$$

Effect of temperature: Prepare several solutions of volume (50 mL) with a concentration of (100 mg/L) for each of (PPD), ( $Pb^{+2}$ ) and ( $Cr^{+3}$ ), add (0.1g) of activated carbon samples, and place them in a vibrating water bath at different temperatures (25,35, and 45 °C) for 2 hours. The solutions were then filtered, and the remaining concentration was measured.

Effect of primary concentration: The influence of concentration and application of isotherms (Langmuir and Freundlich) was studied by producing numerous solutions with a volume of (50 mL) and varied concentrations (100,300,500, and 700 mg/L) of (PPD), ( $Pb^{+2}$ ) and ( $Cr^{+3}$ ), as well as (0.1g) of carbon samples, The activator was placed in a vibrating water bath at (25°C) for 2 hours, after which the solutions were filtered and the concentration after adsorption was determined, and the quantity of adsorption at each concentration was estimated using the equation below [13].

$$Q_e = \frac{(C_0 - C_e)V}{m_{ac}}$$

### 2.3 Preconcentration

Batch method: Prepare three standard solutions of (PPD), ( $Pb^{+2}$ ) and ( $Cr^{+3}$ ), in various volumes (300,600, and 900 mL) at a concentration of (1.0 mg/L) and at pH = 6, then add (1.0 g) of activated carbon and mixed continuously at room temperature for 2 hours. The lead content in the filtrate was determined using an atomic absorber after the solution was filtered.

Column method: Activated carbon was placed within an appropriate separation column with a diameter of 2 cm and a height of 40 cm, and it was positioned between two layers of fiberglass with a height of 3 cm. at room temperature The residual (PPD), ( $Pb^{+2}$ ) and ( $Cr^{+3}$ ), in the solution were determined from the column at room temperature at a flow rate of (3 mL) per minute.

## 3. Results and discussion

### 3.1 Define surface functions

Infrared spectroscopy: (FT-IR) of the raw material revealed a wide band at (3282cm<sup>-1</sup>) elongation back to Vibration of the OH group of polymeric compounds in alcohols or carboxylic acids, and a bundle at (2900 cm<sup>-1</sup>) vibration deformation belongs to alpha CH, and a bundle at (1700cm<sup>-1</sup>) and (1100cm<sup>-1</sup>) vibration deformation belongs to the group C=O and C-O respectively in the carbonyl group or presence of carboxylic. Alkenes have a band at (1600 cm<sup>-1</sup>) owing to C=C expansion vibration, and carboxylic acids have bands at (1205 cm<sup>-1</sup>) and (1027 cm<sup>-1</sup>) due to OH bending vibration and CO expansion, respectively [16]. The beam positions of active groups such as OH and C=O changed and some of them disappeared in the FT-IR spectrum of activated carbon samples obtained after treating the raw material with nitric acid and burning at different temperatures, due to the structural change of the raw material's surface and the formation of other additional functional groups, which leads to changing the vibrations of the bonds at different temperatures [17]. When subjected to high temperatures, the original carbon structure was changed into polycyclic aromatic structures, resulting in a widening of the interlayers between the crystals of activated carbon [18]. We detect a considerable shift in the location of the bundles for several functional groups following adsorption of (PPD), ( $Pb^{+2}$ ), and ( $Cr^{+3}$ ) on activated carbon, and the OH functional group band vanished, indicating that these functional groups contributed considerably to the adsorption process. The location of the functional group beams shows that an ion exchange has occurred between the adsorbent's ions and the functional groups on

the activated carbon surface, especially the OH and C=O groups [15].

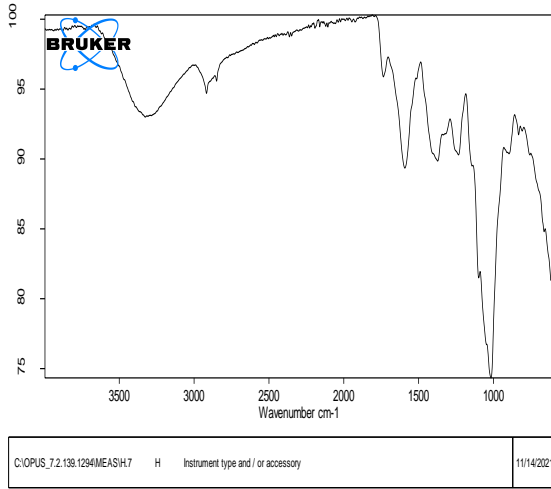


**Figure (1)** FT-IR spectrum of the raw material

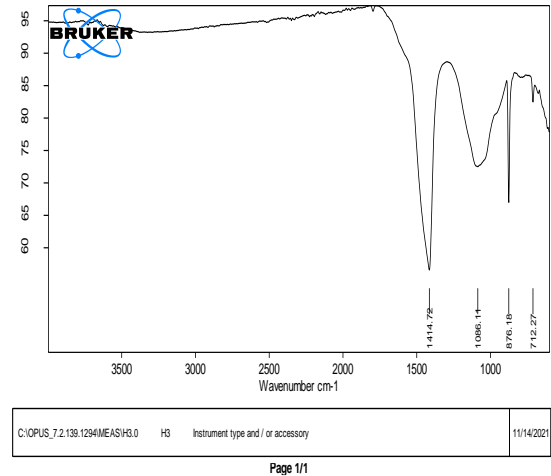


**Figure (2)** FT-IR of (CHN3) before adsorption

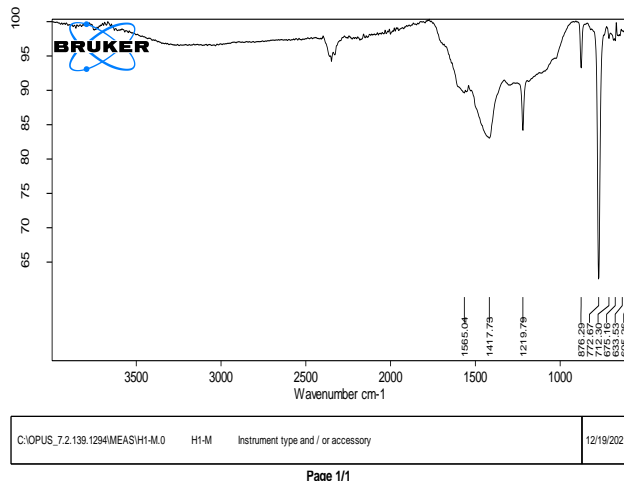


**Figure (3)** FT-IR of (CHN3) after **PPD** adsorption

Scanning electron microscopy: The surface formation of the raw material and the manufactured activated carbon before and after adsorption was studied using a scanning electron microscope (SEM). The contains many pores and gaps of various sizes and shapes, as these pores can provide excellent surfaces for adsorption of pollutants particles, and the reason for their availability is due to the change in functional groups at high temperatures, as well as the evaporation of volatile compounds present [19]. We can see from (SEM) pictures that the structural formation of (CHN3) before and after adsorption (PPD), (Pb+2), and (Cr+3) has changed substantially and that most of the wide holes and gaps have been filled and covered with particles of adsorbent materials.



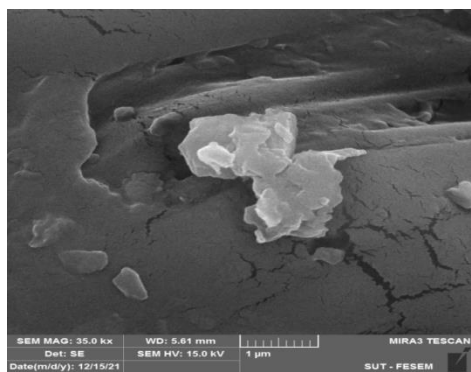


**Figure (4)** SEM of the raw material

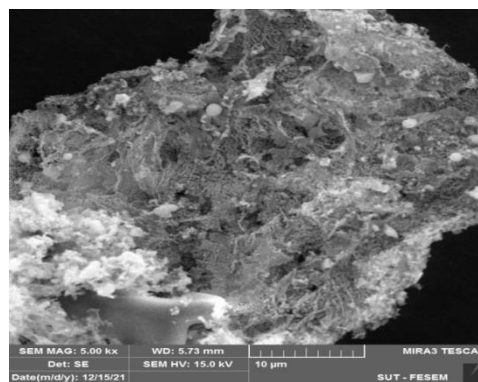


**Figure (5)** SEM of (CHN3) before adsorption

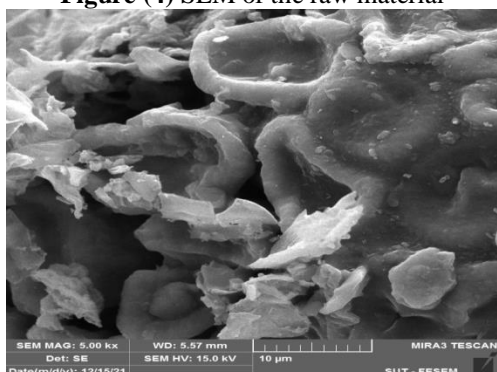


**Figure (6)** SEM of (CHN3) after adsorption of PPD

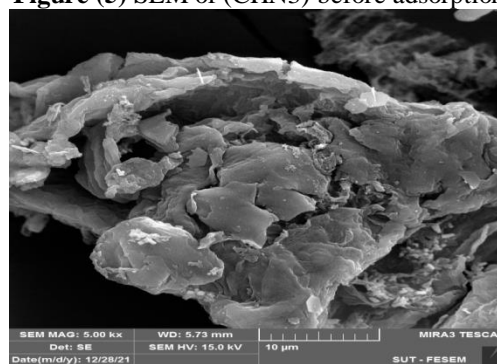


**Figure (7)** SEM of (CHN3) after adsorption of  $Pb^{+2}$

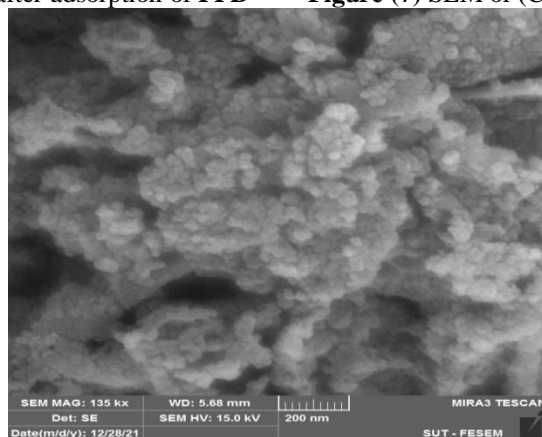


**Figure (8)** SEM of (CHN3) after adsorption of  $Cr^{+3}$

### 3.2 Ash content and moisture

Ash is an inorganic material that acts as an impurity on the surface, clogging the pores and reducing the adsorbent surface area [11]. When compared to activated carbon with nitric acid, the activated carbon includes a very tiny proportion of ash, which improves the carbon's quality, and the ash percentage increases as the activator increases. The moisture content ranged from 1.0 percent to 5.4%, indicating that the activated carbon prepared for the various models does not readily absorb moisture and serving as an indicator of the quality of the activated carbon obtained, particularly activated carbon with nitric acid, where the ratio was between 1 percent and 2 percent. These data also showed how easily activated carbon may be stored.

**Table (1)** values of ash content and moisture

AC	C HN1	C HN2	C HN3	C HN4	C HN5
Ash content %	2	2	2	6	10
Moisture content%	3.8	5.2	5.4	2.0	1.0

### 3.3 Iodine and methylene blue index

The results in Table 2 show that the iodine value increases as the activator concentration increases, that activated carbon with nitric acid has the best iodine adsorption capabilities up to (720 mg/g), and that activated carbon models with iodine values between 500 and 1500 are recommended for the removal of fine pollutants [20]. The blue methylene index for activated carbon with nitric acid increases as the activation level rises. The blue methylene index falls as activation increases, and the proportion of particles removed is quite high, indicating that activated carbon has a high effectiveness in removing both big and tiny particles.

**Table (2)** values of iodine and methylene blue index

AC	C HN1	C HN2	C HN3	C HN4	C HN5
<b>Iodine values(mg/g)</b>	507	634	720	571	380
<b>M.B values(mg/g)</b>	24, 810	24, 910	24, 960	24, 930	24, 810

pH of the zero charge point (pH pzc): Knowing the pH value at which the adsorbent surface is neutral requires determining the acidic function at (pH pzc). The charge of the adsorbent surface is negative when the pH value is more than (pH pzc), and it is positive when the pH value is less than (pH pzc). Thus, the adsorption efficiency of pollutants with a positive charge at pH more than (pH pzc) and the adsorption efficiency of pollutants with a negative charge at pH less than (pH pzc) is improved (pH pzc) [21] By identifying the points of intersection between the curves pH<sub>i</sub> and ΔpH, pH pzc values were obtained.

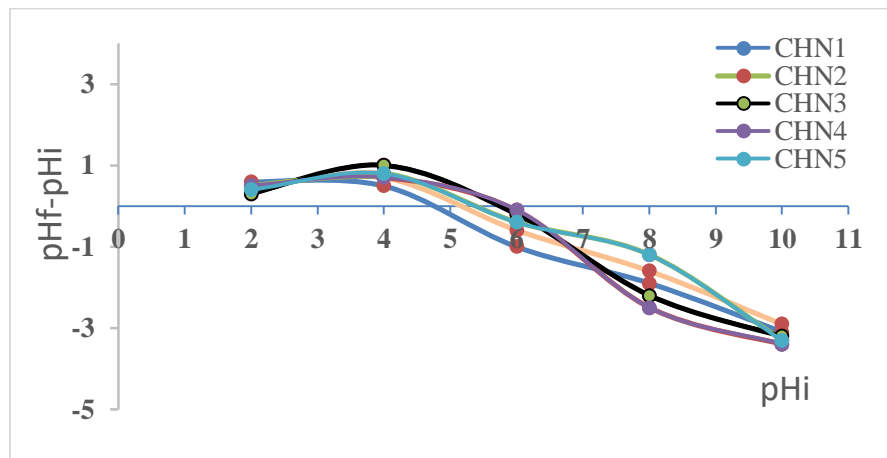


**Figure (9)** shows the (pH pzc) of the activated carbon samples

**Table (3)** shows the values of (pH pzc)

AC	C HN1	C HN2	C HN3	C HN4	C HN5
<b>pH PZC</b>	4.8	5.2	6.0	5.4	4.8

### 3.4 Factors Affecting Adsorption

Adsorbent mass: Figure (10) show that the percentage of adsorption increases as the mass of the adsorbent surface increases and continues to increase until it reaches close values, and the reason for this is that as the surface area of the adsorbent increases, so does the number of functional sites for the bond. With the adsorbent

material and continue Increase the adsorbent dosage until a coating of ions covers the surface, blocking adsorption again [22].

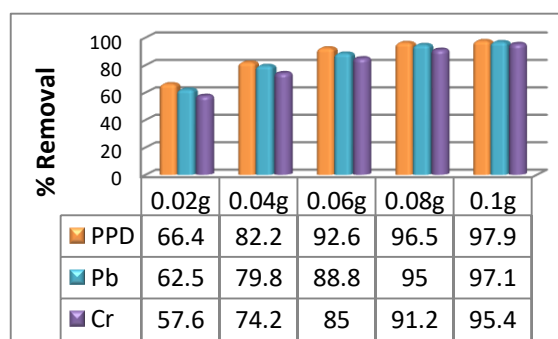
### 3.5 The effect of contact time

Figure (11) illustrate that adsorption happens quickly within the first 60 minutes, and the explanation for this is because the adsorbent material's outer surface has a large number of unoccupied adsorption sites, which allows for fast adsorption during that time period. After 60 minutes, we see that the adsorption rate has dropped and the process has slowed as the adsorption sites on the surface have achieved saturation, resulting in a reduction in the number of adsorption sites as well as the number of unadsorbed molecules. (16,19). The equilibrium time for activated carbon with nitric acid (CHN3) was 120 minutes, according to the findings. Activated carbon with nitric acid, on the other hand, gave larger pores.

The effect of temperature: The percentage of adsorption increases with increasing temperature, as shown in Figure (12). This can be explained by the fact that increasing temperature causes a decrease in the viscosity of the solution, as well as the liberation of functional aggregates, which increases the pores on the surface. The adsorbent material, as well as the increased rate of diffusion of adsorbent molecules on the surface of the adsorbent material. The adsorbent material's kinetic energy increases as temperature rises, and there's a chance that an absorption process may occur concurrently with the adsorption process, which is known as saturation and signifies that the adsorption and absorption processes will occur simultaneously [23].

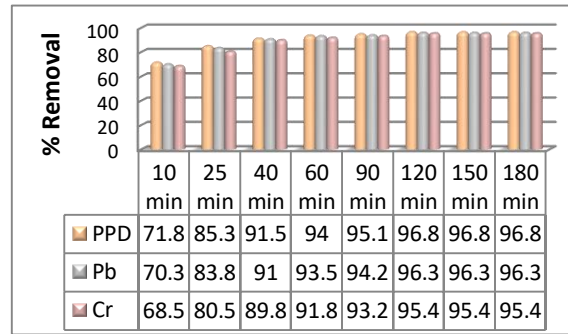
### 3.6 The effect of the initial concentration

Figure (13) demonstrate that when the starting concentration was increased, the percentage of adsorption dropped, with the maximum adsorption rate occurring at the lowest concentration of 100 mg/l. The reason for this is because most of the empty adsorption sites on the adsorbent's surface are Saturated, resulting in increased competition amongst adsorbent molecules and a reduction in adsorption rate at high concentrations [24]. Although the percentage of adsorption decreases as the initial concentration rises, the adsorption capacity  $Q_e$  rises as the initial concentration of the adsorbent rises. Substance particles adsorbed on the adsorbent surface [25].



**Figure (10)** Effect of (CHN3) mass on the removal rate





**Figure (11)** Effect of contact time on the percentage of removal on the surface of (CHN3)

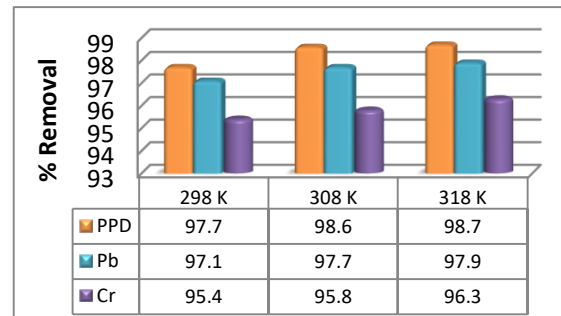


**Figure (12)** Effect of heat on the percentage of removal on the surface of (CHN3)

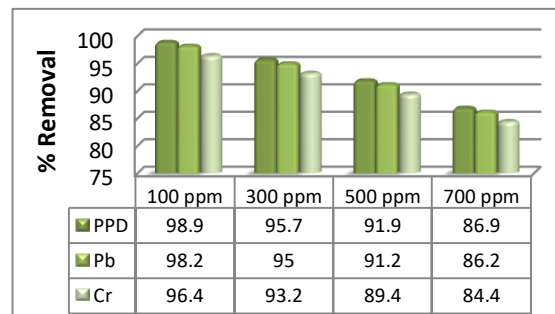


**Figure (13)** Effect of concentration on the percentage of removal on the surface of (CHN3)

Langmuir isotherm: The linear Langmuir equation was utilized to apply the adsorbents' practical adsorption findings to the two utilised adsorbent surfaces.

$$\frac{C_e}{Q_e} = \frac{1}{Q_{max} \cdot K_l} + \frac{C_e}{Q_{max}}$$

The slope and cut-off of the linear connection between  $C_e$  against  $C_e/Q_e$  were used to get the values of  $Q_{max}$  and  $K_l$ .

Friending isotherm: The linear Freundlich equation was utilized to apply the adsorbents' practical adsorption findings to the utilised adsorbent surfaces [26].

$$\ln Q_e = \ln K_f + \frac{1}{n} \ln C_e$$

The slope and cutoff linear connection between  $\ln Q_e$  and  $\ln C_e$  were used to calculate the Freundlich constants  $n$  and  $K_f$ , as well as the value of the correlation coefficient  $R^2$  for the adsorption process.

**Table (4)** Freundlich and Langmuir constants on the surface of CHN3

Adsorbent	Langmuir			Freundlich		
	$R^2$	$Q_{\max}$	$k_l$	$R^2$	$n$	$k_f$
PPD	0.9832	357.1	0.051	0.9937	2.1	36864
$Pb^{+2}$	0.9861	357.1	0.041	0.9891	1.9	29437
$Cr^{+3}$	0.9906	384.6	0.026	0.9969	1.8	21952

The results in Table (4) show that the Langmuir adsorption equation, which produced high linear correlation coefficients between the diverse adsorption processes on the constructed adsorbent surfaces, applies to them in part (0.9906-0.9832). Also, the Freundlich equation applies to it, where it gives linear correlation coefficients between (0.9969-0.9891). We notice that the values of  $n$  denoting adsorption intensity were more than one, indicating that the adsorption is physical, as if ( $n=1$ ) represents chemical adsorption and ( $n>1$ ) means physical adsorption [23].

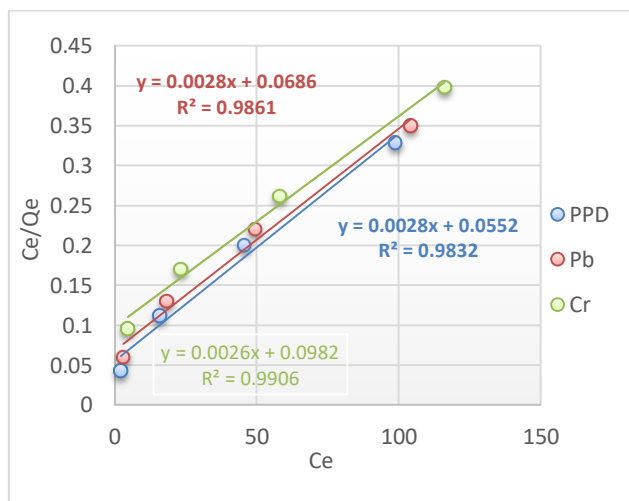


**Figure (14)** Langmuir isotherm to remove ( $Pb^{+2}$ ), ( $Cr^{+3}$ ) and (PPD) on the surface of CHN3

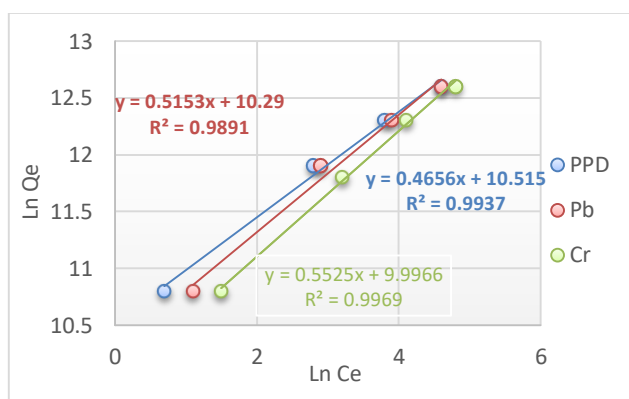


**Figure (15)** Freundlich isotherm to remove ( $Pb^{+2}$ ), ( $Cr^{+3}$ ) and (PPD) on the surface of CHN3

Thermodynamic: The thermodynamic functions of the adsorption processes of ( $Pb^{+2}$ ),  $Cr^{+3}$ , and (PPD) were estimated. From aqueous solutions utilizing activated carbon and nitric acid (CHN3). The values of the

adsorption enthalpy ( $\Delta H$ ) and adsorption entropy ( $\Delta S$ ) were computed using the Vant Hoff equation [21].

$$\ln K = \frac{\Delta S}{R} - \frac{\Delta H}{RT} \quad , \quad K = \frac{Q_e}{C_e}$$

The slope and cut-offs of the straight line equation were calculated from the graph of  $\ln k$  vs.  $1/T$ , and the values of  $\Delta H$  and  $\Delta S$  were calculated from the slope and cut-offs of the straight line equation, respectively. Kibs' mathematical equation was also used to compute the value of the free energy G.

$$\Delta G = \Delta H - T \cdot \Delta S$$

Table (6) show that the heat of adsorption ( $\Delta H$ ) is positive, indicating that all adsorption processes are endothermic, and that all values were less than (40 kg/mol), that adsorbent surfaces is physical. 23 Negative (G) values suggest that adsorption processes happen on spontaneously. The positive values of ( $\Delta S$ ) imply that the adsorbed molecules are less regular on the adsorbing surface than they are in the solution.

**Table (6)** Thermodynamic functions of adsorption on the surface of CHN3

T <sub>K</sub>	PPD			Cr+3			Pb <sup>+2</sup>		
	$\Delta G$	$\Delta H$	$\Delta S$	$\Delta G$	$\Delta H$	$\Delta S$	$\Delta G$	$\Delta H$	$\Delta S$
298	-25.02	+12.23	125.6	-22.8	+7.7	102.6	-24.03	+11.04	118.2
308	-26.6			-23.9			-25.5		
318	-27.9			-25.03			-26.7		

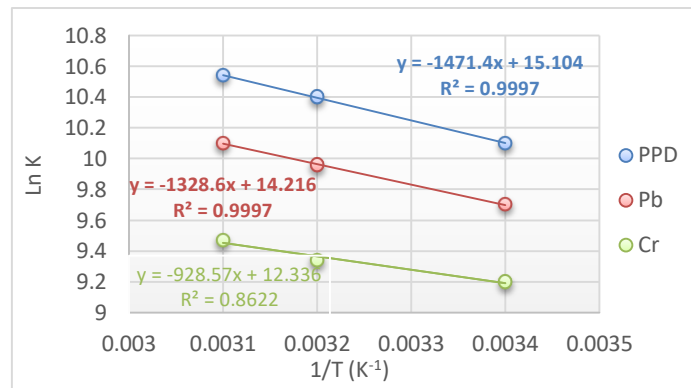


**Figure (16)** Vant-Hof Relationship for the removal of Pb<sup>+2</sup>, (Cr<sup>+3</sup>) and PPD on the surface of CHN3

Batch method: According to the data given in Table 7, The concentration of Cr+3 ion in the leachate solution is (0.0 mg/l), Which confirms that the process of adsorption concentration by the Batch method is one of the important methods that can be applied to get rid of the small concentrations of different elements.

**Table (7)** percentages of removal of (Cr<sup>+3</sup>) using activated carbon by a Preconcentration method in the Batch

	CHN3			
	V (mL)	200	500	800
Con (mg/L)	1.0	1.0	1.0	1.0
% R	100	100	100	100

Column method: The findings demonstrate that the concentration of Chromium ion in the solution descending from the column is equal to (0.0mg/l), as stated in Table 8. This demonstrates that using column

Preconcentration to remove tiny ion concentrations from huge amounts of water is quite beneficial. In comparison to the height of the coal inside the column (3 cm), the flow rate was (3 ml) per minute, implying that for every 1 ml of flow, the height of the coal inside the column was 1 cm, and the flow rate could be raised by raising the height of the coal.

**Table (8)** percentages of ( $\text{Cr}^{+3}$ ) removal using activated carbon by column Preconcentration method

Adsorbent	V (L)	Con.(mg/L)	R%
CHN3	3.0	1.0	100

#### 4. CONCLUSIONS

-Activated carbon was prepared using Bitter Melon, and treated with nitric acid to increase its efficiency in the adsorption process.

-Surface diagnostics using FT-IR and FE-SEM technology

-The adsorption capacity of  $\text{Cr}^{+3}$ ,  $\text{Pb}^{+2}$  and PPD dye was determined by activated carbon with nitric acid (CHN3). It was found that the adsorption capacity of  $\text{Cr}^{+3}$ ,  $\text{Pb}^{+2}$  and dye increases with time, where it is greater at the time (180) mins. Also, the adsorption capacity of PPD dye is greater which in turn is greater than  $\text{Cr}^{+3}$  and  $\text{Pb}^{+3}$  over time when using the two surfaces.

#### 5. References

- [1] Abdel-Fattah, T. M., Haggag, S. M. S. and Mahmoud, M. E. (2011) 'Heavy metal ions extraction from aqueous media using nanoporous silica', *Chemical Engineering Journal*, 175(1), pp. 117–123. doi: 10.1016/j.cej.2011.09.068.
- [2] Elliott, Elise G., et al. "A systematic evaluation of chemicals in hydraulic-fracturing fluids and wastewater for reproductive and developmental toxicity." *Journal of exposure science & environmental epidemiology* 27.1 (2017).
- [3] D. C. Muir, G. Howard, P. H. Are there other persistent organic pollutants? A challenge for environmental chemists. *Environ. Sci. Technol.* (2006).
- [4] Scheringer, M. (2009) 'Long-range transport of organic chemicals in the environment', *Environmental Toxicology and Chemistry. Environ Toxicol Chem*, pp. 677–690. doi: 10.1897/08-324R.1.
- [5] Undeman, Emma, Stellan Fischer, and Michael S. McLachlan. "Evaluation of a novel high throughput screening tool for relative emissions of industrial chemicals used in chemical products." *Chemosphere* 82.7 (2011).
- [6] Nahar, Mst Nur-E-Nazmun. "Role of Proline in Tobacco Cultured Cells Under Arsenate Stress." (2017).
- [7] T. Brown, N. Wania, F. "Screening chemicals for the potential to be persistent organic pollutants: A case study of Arctic contaminants. *Environ. Sci.*2008.
- [8] M.M. Hassan, C.M. Carr A critical review on recent advancements of the removal of reactive dyes from dyehouse effluent by ion-exchange adsorbents *Chemosphere*, 209 (1) (2018).

- [9] Patel, Priti N. "Methylene blue for management of ifosfamide-induced encephalopathy." *Annals of Pharmacotherapy* 40.2 (2006): 299-303.
- [10] P. Egeghy, P. Judson, R. Gangwal, S.; Mosher, S.; Smith, D.; Vail, J.; Cohen Hubal, E. A. "The exposure data landscape for manufactured chemicals. *Sci. Total* " (2012).
- [11] Mamane, Ousmaila Sanda, et al. "Préparation et caractérisation de charbons actifs à base de coques de noyaux de Balanites Eagyptiaca et de Zizyphus Mauritiana." *J. Soc. Ouest-Afr. Chim* 41 (2016).
- [12] Nunes, Cleiton A., and Mário C. Guerreiro. "Estimation of surface area and pore volume of activated carbons by methylene blue and iodine numbers." *Química Nova* 34.3 (2011).
- [13] Obaid, Saba A. "Removal chromium (VI) from water by magnetic carbon nano-composite made by burned straw." *Journal of Physics: Conference Series*. Vol. 1234. No. 1. IOP Publishing, 2019.
- [14] Mansur, Noor Fhadzilah, Megat Ahmad Kamal Megat Hanafiah, and Mardhiah Ismail. "Adsorption of Pb (II) ions on sulfuric acid treated leucaena leucocephala leaf powder." *MATEC Web of Conferences*. Vol. 27. EDP Sciences, 2015.
- [15] Shandi, Saba Golshan, Faramarz Doulati Ardejani, and Fereydoun Sharifi. "Assessment of Cu (II) removal from an aqueous solution by raw Gundelia tournefortii as a new low-cost biosorbent: Experiments and modelling." *Chinese Journal of Chemical Engineering* 27.8 (2019).
- [16] Shouman, Mona Abdel Hamid, and Soheir Abdel Atty Khedr. "Removal of Cationic Dye from Aqueous Solutions by Modified Acid-Treated Pomegranate Peels (PUNICA GRANATUM): Equilibrium and Kinetic Studies." *Asian Journal of Applied Sciences* 3.4 (2015).
- [17] Chen, Hao, et al. "Removal of copper (II) ions by a biosorbent—Cinnamomum camphora leaves powder." *Journal of Hazardous Materials* 177.1-3 (2010).
- [18] Glaser, Bruno, et al. "The Terra Preta phenomenon: a model for sustainable agriculture in the humid tropics." *Naturwissenschaften* 88.1 (2001).
- [19] Bello, Olugbenga Solomon, et al. "Rhodamine B dye sequestration using Gmelina aborea leaf powder." *Heliyon* 6.1 (2020).
- [20] Alhamed, Yahia A. "Adsorption kinetics and performance of packed bed adsorber for phenol removal using activated carbon from dates' stones." *Journal of hazardous materials* 170.2-3 (2009).
- [21] Mohammed, Ahmed A., et al. "Simultaneous adsorption of tetracycline, amoxicillin, and ciprofloxacin by pistachio shell powder coated with zinc oxide nanoparticles." *Arabian Journal of Chemistry* 13.3 (2019).
- [22] Nisreen, A. J., and M. M. Sirhan. "Comparative study of removal pollutants (Heavy metals) by agricultural wastes and other chemical from the aqueous solutions." *Iraqi Journal of agricultural sciences* 52.2 (2021).

[23] Al-abady, Faiz Mohsen, Nashwan Omar Tapabashi, and Afnan Najdat Bahjat. "Study of thermodynamic and kinetic adsorption of azo dyes on different adsorbent surfaces." *kirkuk university journal for scientific studies* 14.2 (2019).

[24] Sabbar, Huda Adil. "Adsorption of Phenol from Aqueous Solution using Paper Waste." *Iraqi Journal of Chemical and Petroleum Engineering* 20.1 (2019).

[25] Shrivastava, V. S. "Removal of Congo red dye from aqueous solution by *Leucaena leucocephala* (Subabul) seed pods." *International Journal of ChemTech Research* 4.3 (2012).

[26] Cao, Qinying, et al. "Potential of *Punica granatum* biochar to adsorb Cu (II) in soil." *Scientific reports* 9.1 (2019).

[27] Kuang, Yu, Xiaoping Zhang, and Shaoqi Zhou. "Adsorption of methylene blue in water onto activated carbon by surfactant modification." *Water* 12.2 (2020).